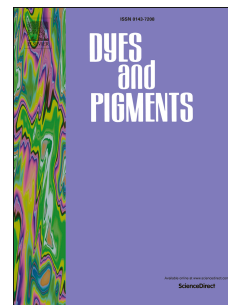


Journal Pre-proof

A mild and sequentially Pd/Cu-catalyzed domino synthesis of acidochromic Indolo[3,2-*a*]carbazoles – Free bases of apocyanine dyes

Patrik Niesobski, Jennifer Nau, Lars May, Alae-Eddine Moubait, Thomas J.J. Müller



PII: S0143-7208(19)31393-2

DOI: <https://doi.org/10.1016/j.dyepig.2019.107890>

Reference: DYPI 107890

To appear in: *Dyes and Pigments*

Received Date: 14 June 2019

Revised Date: 7 August 2019

Accepted Date: 16 September 2019

Please cite this article as: Niesobski P, Nau J, May L, Moubait A-E, Müller TJJ, A mild and sequentially Pd/Cu-catalyzed domino synthesis of acidochromic Indolo[3,2-*a*]carbazoles – Free bases of apocyanine dyes, *Dyes and Pigments* (2019), doi: <https://doi.org/10.1016/j.dyepig.2019.107890>.

This is a PDF file of an article that has undergone enhancements after acceptance, such as the addition of a cover page and metadata, and formatting for readability, but it is not yet the definitive version of record. This version will undergo additional copyediting, typesetting and review before it is published in its final form, but we are providing this version to give early visibility of the article. Please note that, during the production process, errors may be discovered which could affect the content, and all legal disclaimers that apply to the journal pertain.

© 2019 Published by Elsevier Ltd.

A Mild and Sequentially Pd/Cu-catalyzed Domino Synthesis of Acidochromic Indolo[3,2-*a*]carbazoles – Free Bases of Apocyanine DyesPatrik Niesobski,^a Jennifer Nau,^a Lars May,^a Alae-Eddine Moubsit,^a and Thomas J. J. Müller^{*,a}^aInstitut für Organische Chemie und Makromolekulare Chemie, Heinrich-Heine-Universität Düsseldorf, Universitätsstrasse 1, D-40225 Düsseldorf, Germany

Email: ThomasJJ.Mueller@hhu.de

*Keywords: Acidochromism; Apocyanine Dyes; Domino Reaction; Fluorescence; Indolo[3,2-*a*]carbazoles; Sequential Catalysis.***ABSTRACT**

A sequentially Pd(II)/Cu(II)-catalyzed dimerization of indoles with subsequent oxidative cycloaromatization with alkynes give rise to the formation of strongly violet to blue solution and solid state emissive indolo[3,2-*a*]carbazoles in a domino fashion under mild conditions and in moderate to good yields. Upon protonation the absorption bands are significantly red-shifted with concomitant quenching of the fluorescence. The site of protonation was scrutinized by NMR studies of the protonated species and confirmed by DFT calculations. The obtained chromophores of the acidochromicity of the title compounds are rarely described apocyanine dyes. The relevant absorption bands can be unambiguously assigned by TDDFT calculations.

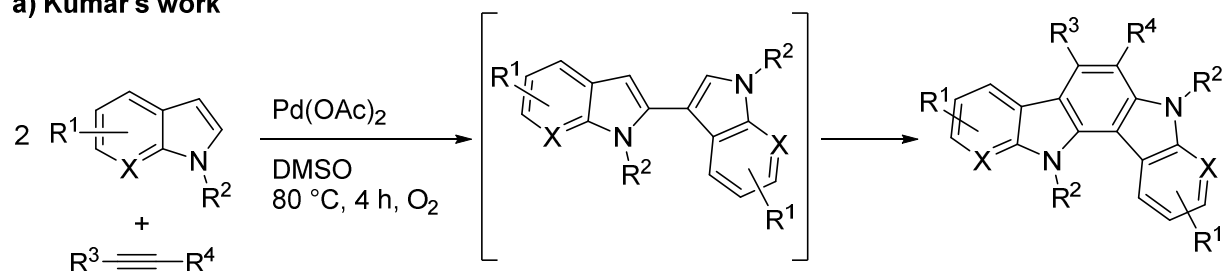
1. Introduction

The steadily growing quest for novel functional organic materials, such as chromophores, fluorophores and electrophores [1], with heterocyclic core structures is an ongoing challenge for synthetic chemistry and in recent years the concepts of multicomponent processes [2] and domino reactions [3] have opened new opportunities for modular syntheses of these targets. These functional π -systems are underlying molecular entities in molecule based electronics such as organic light-emitting diodes (OLEDs) [4], dye-sensitized solar cells (DSSCs) [5], and organic photovoltaics (OPVs) [6], or bio and environmental analytics [7]. Particularly interesting are sensitive dyes which undergo changes in their absorption and/or emission properties by external stimuli such as light [8], heat [9], current [10], mechanical pressure [11], solvent polarity [12] or pH changes [13]. The latter phenomenon is called halo- or acidochromism founding the principle of pH indicators [14] and smart inks [15]. In addition, fluorohalochromic dyes, which are both fluorescent and halochromic have as dual readout chromophores advantages such as high sensitivity and fast read-outs using relatively simple and inexpensive instruments, for instance by ratiometric intensity analysis at a certain wavelengths [16]. With respect to intensity, for instance fluorescent chemosensors, in particular fused nitrogen heterocycles, are either quenched (turn OFF) or induced (turn ON) upon protonation.

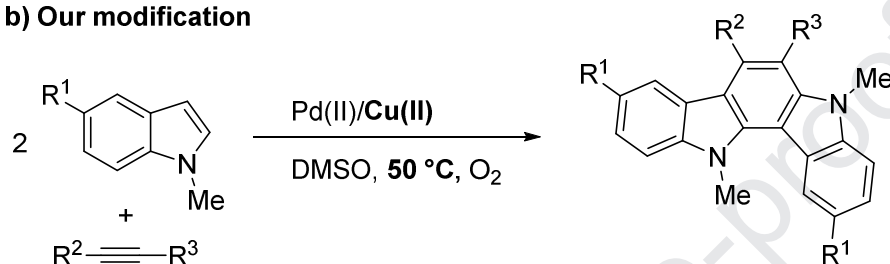
First indolocarbazoles [17] were first mentioned in the late 1950s [18], but received attention only 30 years later, when biologically active natural products such as the alkaloids K-252a [19] or staurosporine [20] were isolated. Ever since this scaffold has not only been used for the development of potential novel drugs [21] but increasingly for conceptualizing functional materials [22]. Out of five possible isomers, indolo[3,2-*a*]carbazoles have scarcely been studied, but in the last few years some methods have been developed starting from hydrazines [23], 2,3-biindolyls [24], and indoles [25]. Very recently, Kumar's group has disclosed a Pd-catalyzed [2 + 2 + 2] annulation of indoles or azaindoles with alkynes, starting with indoles dimerization to give 2,3-biindolyls, which subsequently cyclizes with alkynes giving indolo[3,2-*a*]carbazoles (Scheme 1a), however, substrates with strongly electron withdrawing groups were not converted [26]. About the same time, motivated by our interest in sequentially bimetallically Pd/Cu-catalyzed processes [27] as a rapid entry to multicomponent syntheses of heterocycles in a one-pot fashion [28], we probed the reaction of indoles and alkynes at

lower temperatures in the presence of Pd(II) and Cu(II) catalysts to give intensively luminescent indolo[3,2-*a*]carbazoles (Scheme 1b).

a) Kumar's work



b) Our modification



Scheme 1. Approaches to the domino synthesis of indolo[3,2-*a*]carbazoles.

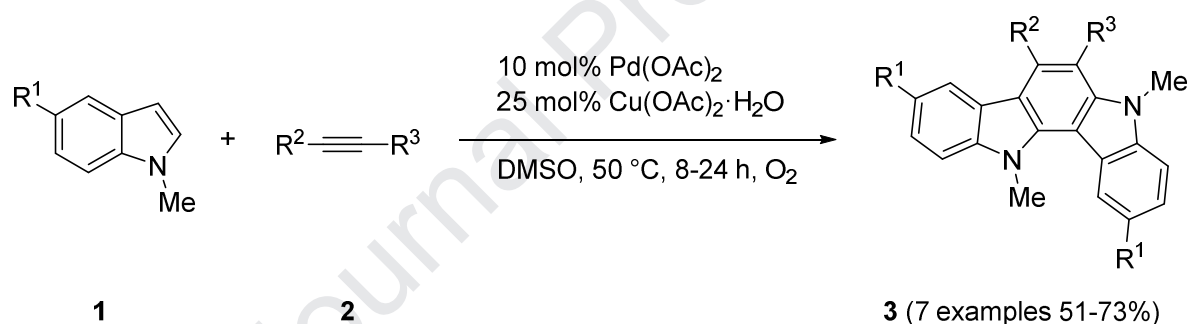
As part of our program to explore diversity oriented one-pot syntheses of functional chromophores by multicomponent [1] and domino reactions [3], we have reported domino syntheses of protochromic “ON–OFF–ON” luminescent 2-styryl quinolines [29] and “OFF–ON” cation-induced fluorescent 2,4-diarylpyrano[2,3-*b*]indoles [30]. Herein, we report a modified pseudo-three-component synthesis of electronically interesting indolo[3,2-*a*]carbazoles, a class of tetracyclic fused indoles and discuss their hitherto unexplored photophysical properties and acidochromicity.

2. Results and discussion

2.1. Synthesis

The reaction of 1-methylindole (**1a**) ($R^1 = \text{H}$) and toluene (**2a**) ($R^2 = R^3 = \text{Ph}$) in DMSO in the presence of catalytic amounts of $\text{Pd}(\text{OAc})_2$ and $\text{Cu}(\text{OAc})_2 \cdot \text{H}_2\text{O}$ as an oxidant under oxygen atmosphere was selected as a model system and optimized (for the optimization, see Supp Inf Table S1). Unlike Kumar's work, whose optimization was initiated at 80 °C by variation of the cooxidant, we started the domino reaction at room temp with a stoichiometric amount of $\text{Cu}(\text{OAc})_2 \cdot \text{H}_2\text{O}$ and then successively increased the reaction temperature and reduced the amount of copper oxidant to find that at 50 °C and

in the presence of catalytic amounts of Cu(II) salts, the best result was achieved, whereas without cooxidant as well as at 80 °C significantly less yield was observed. Kumar, on the other hand, who had also experimented with Cu(OAc)₂, found out that omitting the cooxidant at 80 °C led to more product but could not reproduce the yield at lower temperatures [26]. As such, we decided to synthesize and discuss only electronically interesting indolo[3,2-*a*]carbazole with our conditions, a modified, milder variant of Kumar's method, and therefore the preparative studies were performed with electron-rich and electron-poor 1-methyl indoles **1** and alkynes **2** to give 5,12-dimethyl-indolo[3,2-*a*]carbazoles **3** in moderate to good yields in the sense of a domino reaction representing a quadruple CH-functionalization (Scheme 2). All title compounds **3** were isolated as colorless solids which fluoresce violet to blue both in solution and in the solid state. The structural assignment was unambiguously corroborated by extensive ¹H and ¹³C NMR and IR spectroscopy, and mass spectrometry, and the molecular composition was verified by combustion analyses.



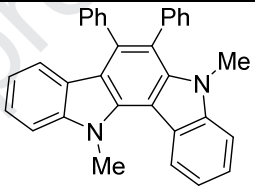
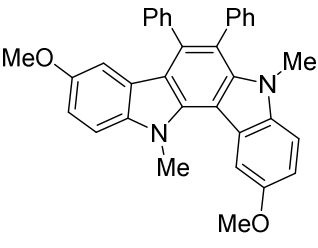
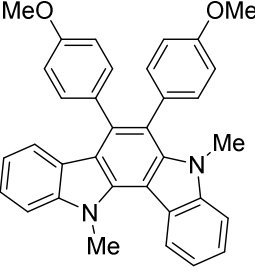
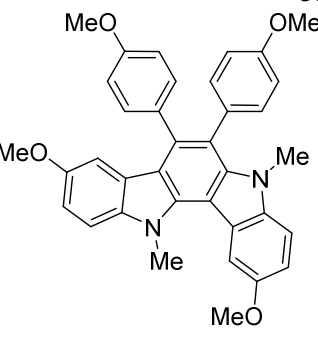
Scheme 2. Pseudo-three-component domino synthesis of indolo[3,2-*a*]carbazoles **3** by oxidative Pd/Cu-catalyzed quadruple CH-functionalization of indoles **1** with alkynes **2**.

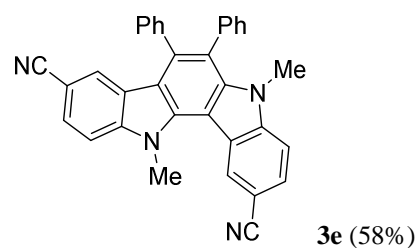
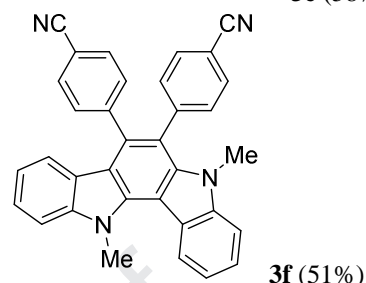
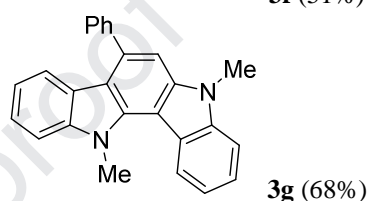
With this protocol electron-donating methoxy substituents can be introduced either via the indole or the alkyne (Table 1, entries 2 and 3), as well as the strongly electron withdrawing cyano groups after a prolonged reaction time of 24 h (Table 1, entries 5 and 6), in contrast to Kumar's method [26]. While the methoxy substituent can be simultaneously incorporated via both starting materials (Table 1, entry 4), this transformation does not work with the cyano group.

In addition to Kumar's work, the triisopropyl-protected alkyne **2d** was selectively transformed into the simply phenylated indolocarbazole **3g** (Table 1, entry 7). To the best of our knowledge, only one method has been developed for 7-phenylindolo[3,2-*a*]carbazoles to date, starting from indoles and β -nitrostyrenes that are reacted with tin and manganese salts for prolonged reaction times to give only

low yields [31]. Here, the selectivity is very likely affected by the steric hindrance of the TIPS substituent which is cleaved off in the course of the reaction. Kumar [26] proposed a mechanistic rationale that commences with an electrophilic palladation, followed by subsequent migration [32], insertion of the second indole and reductive elimination [33] to form 2,3-biindolyls. The subsequent palladium-catalyzed oxidative cycloaromatization of the intermediate with alkyne via dual CH-activation leads to the title compounds **3** [24]. In our approach, the addition of catalytic amounts of copper acetate allows to lower the reaction temperature, presumably due to a more efficient reoxidation of the palladium catalyst, comparable to Wacker oxidations [34].

Table 1. Pseudo-three-component domino synthesis of indolo[3,2-*a*]carbazoles **3**.

entry	indole 1	alkyne 2	indolo[3,2- <i>a</i>]carbazole 3 (yield) ^[b]
1 ^[c]	R ¹ = H (1a)	R ² = R ³ = Ph (2a)	 3a (72%)
2 ^[c]	R ¹ = OMe (1b)	2a	 3b (73%)
3 ^[c]	1a	R ² = R ³ = <i>p</i> -MeOC ₆ H ₄ (2b)	 3c (68%)
4 ^[c]	1b	2b	 3d (60%)

5^[d] R¹ = CN (**1c**)**2a**6^[d]**1a**R² = R³ = *p*-NCC₆H₄ (**2c**)7^{[c][e]}**1a**R² = Ph, R³ = Si^{*i*}Pr₃ (**2d**)

[a] Reaction conditions: indole **1** (0.50 mmol), alkyne **2** (0.25 mmol), Pd(OAc)₂ (0.05 mmol), Cu(OAc)₂ · H₂O (0.125 mmol), DMSO (5 mL), 50 °C under O₂. [b] Isolated yield. [c] Reaction time: 8 h. [d] Reaction time: 24 h. [e] 0.50 mmol of **2d**.

2.2. Photophysical properties

Already previous studies on substituted indolo[3,2-*a*]carbazoles indicated interesting photophysical properties [24]. With a small library of 5,12-dimethyl-indolo[3,2-*a*]carbazoles in hand we decided to assess the substitution effects on the optical properties. All derivatives were characterized by quantitative absorption and emission spectroscopy as well as relative fluorescence quantum yields Φ_F were determined (Table 2).

Table 2. Selected photophysical properties of indolo[3,2-*a*]carbazoles **3** (recorded in CH₂Cl₂ at *T* = 293 K).

entry	compound	$\lambda_{max,abs}$ [nm] (ϵ [L·mol ⁻¹ ·cm ⁻¹]) ^[a]	$\lambda_{max,em}$ [nm] (Φ_F) ^[c]	Stokes shift $\Delta\tilde{\nu}$ [cm ⁻¹] ^[d]
1	3a	250 (41100), 295 (53600), 354 (10100), 370 (16000)	390 (0.50)	1400
2	3b	253 (47400), 282 (44700), 311 (41200), 349 (11400), 365 (14900)	395 (0.45)	2100
3	3c	253 (46100), 296 (59100), 354 (11000), 370 (17600)	389 (0.52)	1300
4	3d	249 (44900), 303 (50700), 365 (10500), 383 (16900)	403 (0.48)	1300
5	3e	298 (80900), 358 (10300), 375 (17100)	391 (0.52)	2400
6	3f	244 (55500), 292 (44400), 355 (11400), 372 (15200)	436 (0.29)	4000
7	3g	251 (39300), 295 (45200), 350 (9200), 366	407 (0.54)	2800

[a] $c(\mathbf{3}) = 10^{-5}$ M. [b] $c(\mathbf{3}) = 10^{-7}$ M, $\lambda_{\text{exc}} = 280$ nm. [c] Recorded at $\lambda_{\text{exc}} = 280$ nm, $c(\mathbf{3}) = 10^{-7}$ M, determined with 2,5-diphenyloxazole as a standard in cyclohexane, ($\Phi_F=1.00$ [35]). [d] $\Delta\tilde{\nu} = \lambda_{\text{max(abs)}}^{-1} - \lambda_{\text{max(em)}}^{-1}$.

Generally, the absorption characteristics of all compounds are quite similar, whereby the longest wavelength absorption band appears at around 370 nm. The compounds **3a-g** show a strong blue luminescence in solution (dichloromethane) (Figure 1), with Stokes shifts in a range from 1300 to 4000 cm^{-1} . The emission maximum of the derivatives **3a-c** and **3e** can all be found at around 390 nm (Figure 2). The tetramethoxy substituted indolo[3,2-*a*]carbazole **3d** is slightly bathochromic shifted emission maximum at 403 nm, also the unsymmetrically substituted indolo[3,2-*a*]carbazole **3g** displays a slight red-shift to 407 nm in comparison to compound **3a**. For the cyano-substituted derivative **3f** substantial bathochromic shift to 436 nm is determined.



Figure 1. Visual impression of indolocarbazoles **3** under daylight (top) and hand-held UV lamp (bottom) in dichloromethane ($c(\mathbf{3}) = 10^{-5}$ M, $\lambda_{\text{exc}} = 365$ nm).

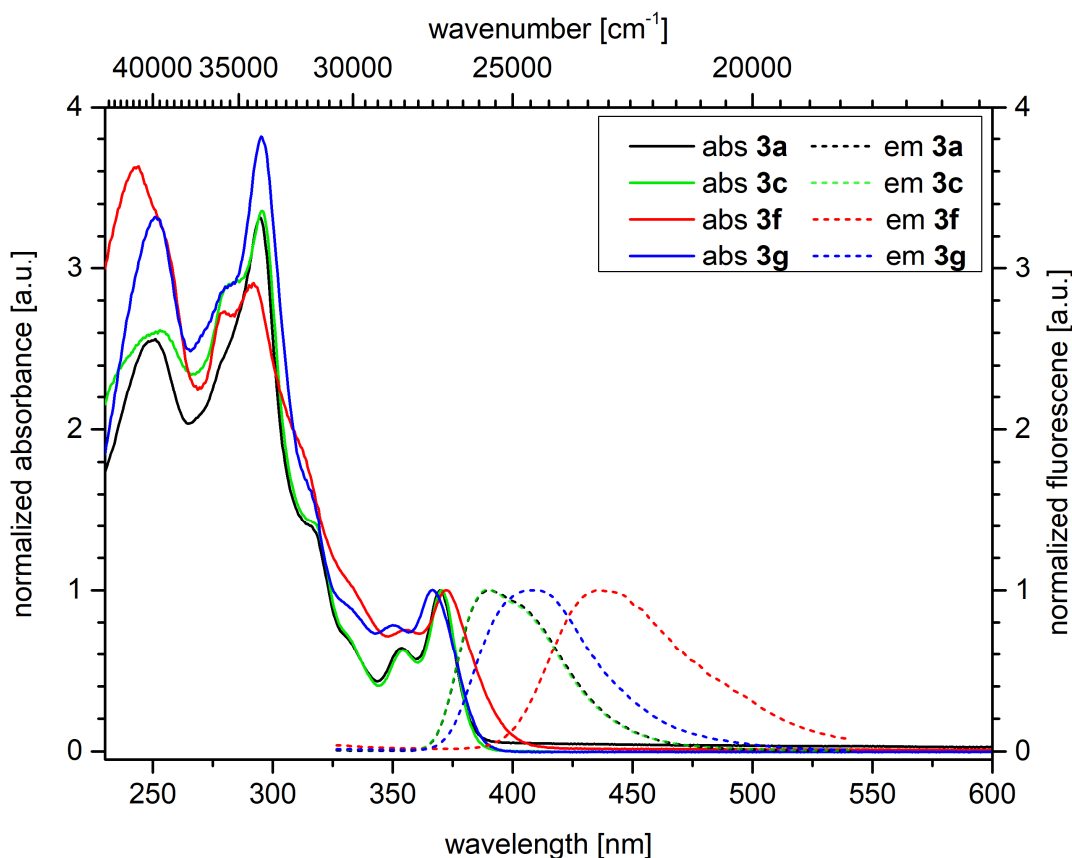


Figure 2. Normalized UV/Vis absorption (recorded in CH₂Cl₂, $T = 293$ K, $c(\mathbf{3}) = 10^{-5}$, bold line) and emission bands (recorded in CH₂Cl₂, $T = 293$ K, $c(\mathbf{3}) = 10^{-7}$, $\lambda_{exc}(\mathbf{3a}) = 294$ nm, $\lambda_{exc}(\mathbf{3c,f,g}) = 280$ nm, dashed line) of indolocarbazoles **3a,c,f,g**.

Furthermore, relative fluorescence quantum yields [36] were measured with 2,5-diphenyloxazole as a standard in cyclohexane ($\Phi_F = 1.00$ [35]). The compounds **3a-e** and **3g** show a similar distinctive fluorescence in dichloromethane with quantum yields ranging from 45 to 54%. Interestingly, only the *p*-cyanophenyl substitution in positions R² and R³ (**3f**) leads to a significant decrease in fluorescence ($\Phi_F = 29\%$).

Most remarkably, the addition of trifluoroacetic acid clearly changes the absorption and emission spectra of the indolocarbazoles **3**, which is a consequence of a selective protonation of the carbazole core (vide infra). This acidochromism was studied by absorption spectroscopy for all indolo[3,2-*a*]carbazoles **3** (Table 3).

Table 3. Comparison of absorption maxima of non-protonated **3** and protonated indolo[3,2-*a*]carbazoles **3-H⁺**.

entry	compound	$\lambda_{max,abs}$ [nm] (ϵ [L·mol ⁻¹ ·cm ⁻¹]) ^[a] 3	$\lambda_{max,abs}$ [nm] (ϵ [L·mol ⁻¹ ·cm ⁻¹]) ^[a] 3-H⁺ ^[b]	acidochromicity shift [cm ⁻¹] ^[c]
1	3a	250 (41100), 295 (53600), 354 (10100), 370 (16000)	277 (31400), 297 (30100), 367 (6300), 479 (12200)	6200
2	3b	253 (47400), 282 (44700), 311 (41200), 349 (11400), 365 (14900)	297 (40500), 363sh (8000), 499 (8300)	7400
3	3c	253 (46100), 296 (59100), 354 (11000), 370 (17600)	278 (27800), 300 (23400), 399sh (5800), 482 (10200)	6300
4	3d	249 (44900), 303 (50700), 365 (10500), 383 (16900)	287sh (25500), 301 (28500), 506 (9000)	6300
5	3e	298 (80900), 358 (10300), 375 (17100)	301 (68700), 358 (10400), 375 (15600)	0
6	3f	244 (55500), 292 (44400), 355 (11400), 372 (15200)	280 (38200), 289 (38500), 372 (11600)	0
7	3g	251 (39300), 295 (45200), 350 (9200), 366 (11800)	277 (21400), 295 (22400), 368 (4300), 466 (9300)	5900

[a] Recorded in CH₂Cl₂, *T* = 293 K, *c* = 10⁻⁵ M. [b] Transferred into the cell (3 mL), addition of 200 μ L trifluoroacetic acid (TFA). [c] $\Delta\tilde{\nu} = \lambda_{max(abs[3])}^{-1} - \lambda_{max(abs[3-H^+])}^{-1}$.

All free bases give colorless solutions, whereby after addition of trifluoroacetic acid (TFA) the methoxy and phenyl derivatives **3a-d** and **3g** became yellow to red solutions (Figure 3). Interestingly, in the protonation studies with cyano-substituted indolo[3,2-*a*]carbazoles **3e** and **3f** no significant change in the absorption spectra was detected. Presumably by strongly electron withdrawing cyano groups their basicity is too low.



Figure 3. Visual color impression of indolocarbazoles **3** under daylight (top) and hand-held UV lamp (bottom) after the addition of TFA (recorded in CH_2Cl_2 , $c(\mathbf{3}) = 10^{-4}$ M, $\lambda_{exc} = 365$ nm).

In all other absorption spectra of the conjugated indolocarbazole salts of **3a-d** and **3g**, a new red-shifted absorption maximum forms between 466 and 506 nm. Thereby the tetramethoxy substituted indolo[3,2-*a*]carbazole **3d** shows the largest bathochromic shift with an absorption maximum at 506 nm. Moreover, the acidochromic shifts of compounds **3a-d** and **3g** range from 5900 (**3g**) to 7400 cm^{-1} (**3b**). The protonation has also an interesting effect on the emission properties of the indolo[3,2-*a*]carbazoles. The fluorescence of all compounds, including the cyano-substituted derivatives, is noticeably quenched after addition of an excess amount of TFA. The process can be reversed by adding triethylamine and all solutions are colorless again as prior to the treatment with TFA, and they fluoresce violet to blue under the hand-held UV lamp.

In addition, we photometrically determined the $\text{p}K_a$ value of the conjugated base of **3a**. Therefore, trifluoroacetic acid was chosen as a suitable acid because it is completely dissociated in dichloromethane. For the $\text{p}K_a$ determination by absorption spectroscopy, the pH-value was

successively lowered from 1.58 to 0.28 and the corresponding absorption spectra were recorded (Figure 4). With successive addition of TFA, the maxima at 354 and 370 nm of **3a** disappear and a new red-shifted maximum at 480 nm was detected for the protonated species **3a-H⁺**. From these titrations a pK_a value of 0.75 for **3a-H⁺** was determined (for experimental details, see Supp Inf).

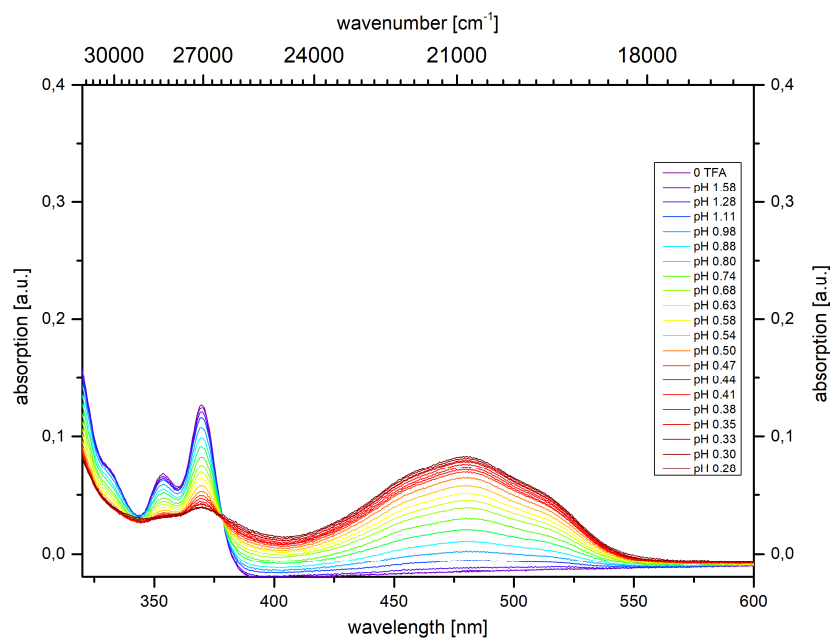


Figure 4. Absorption spectra of **3a** in the presence of increasing amounts of TFA (recorded in CH₂Cl₂, $c(\mathbf{3a}) = 10^{-5}$ m, $T = 293$ K).

Furthermore, the fluorescence quenching of **3a** after addition of trifluoroacetic acid was quantitatively monitored (Figure 5).

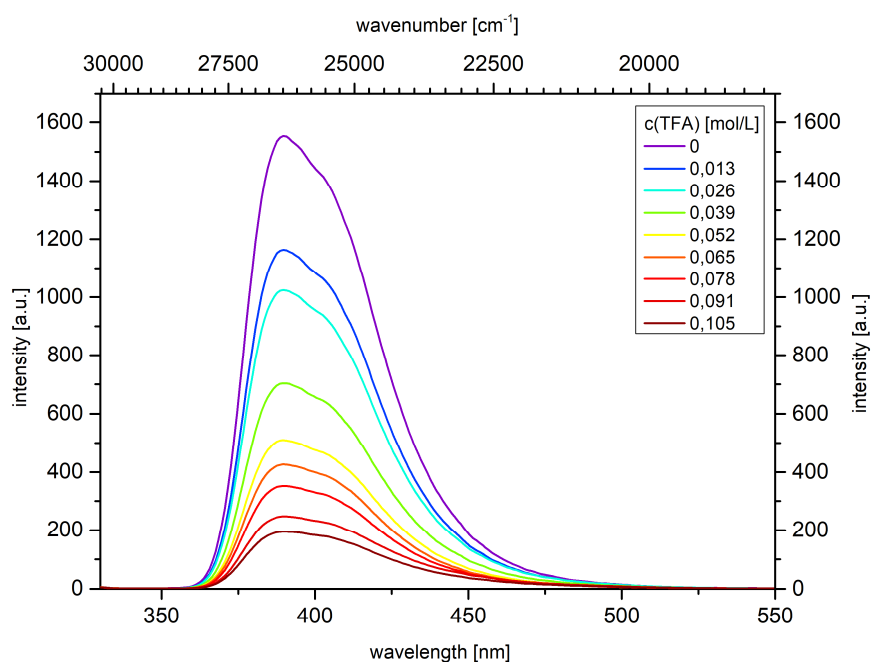


Figure 5. Emission spectra of **3a** in the presence of increasing aliquots of TFA (recorded in CH_2Cl_2 , $c(\mathbf{3a}) = 10^{-7}$ M, $T = 293$ K, $\lambda_{exc} = 294$ nm).

The Stern-Volmer plot of F_0/F against the concentration of TFA reveals a linear correlation (Figure 6) and the Stern-Volmer constant K_{sv} was determined to 49.940 Lmol^{-1} . The Stern-Volmer constant K_{sv} correlates by definition of steady-state quenching to the $\text{p}K_a$ value of **3a**. The $\text{p}K_a$ is calculated therefrom to 1.97, which is in reasonably good agreement with $\text{p}K_a$ value determined by absorption spectroscopy.

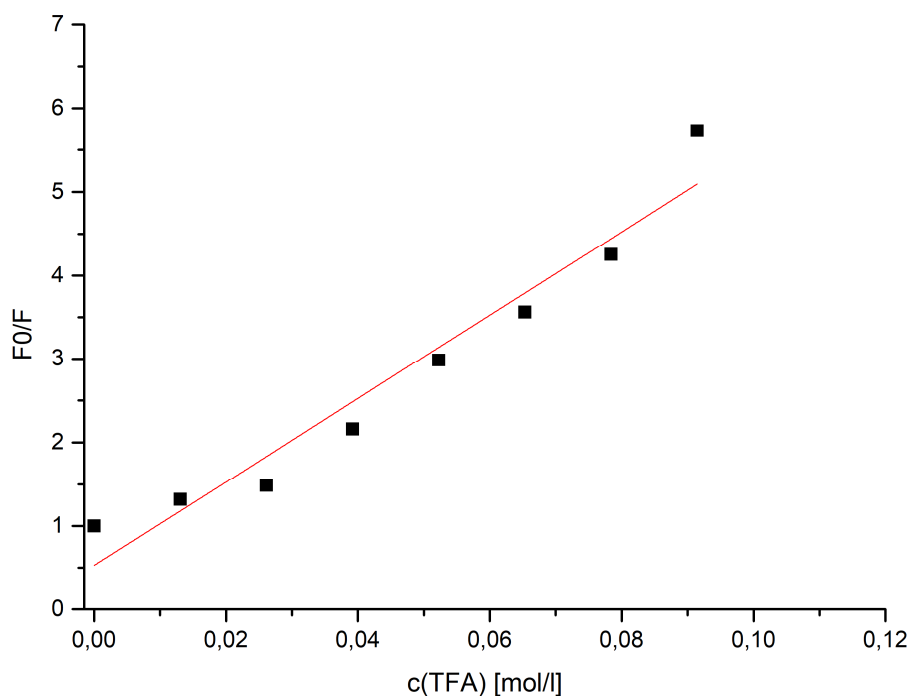


Figure 6. Stern-Volmer plot of **3a** ($c_0(\mathbf{3a}) = 10^{-7}$ m in CH_2Cl_2 , $T = 293$ K, $\lambda_{\text{max}(em)} = 390$ nm; $F_0/F = 0.52932 + 49.904[\text{H}^+]$; $r^2 = 0.97826$).

2.3. NMR protonation studies

Intrigued by the observed acidochromicity of the title compounds **3**, NMR studies were performed to localize the protonation site of indolo[3,2-*a*]carbazoles **3**. The ^1H NMR spectra of **3a** and **3a-H⁺** reveal that upon protonation only a single new species was formed, supported by the appearance of a single set of signals, accompanied by an additional singlet at δ 5.37 arising from the trifluoroacetic acid proton (Figure 7). 2D NMR experiments, such as NOESY and HMBC, allowed the unambiguous assignment of position 6 as the site of protonation (for details and spectra, see Supp Inf). In principle, most of the signals of the protonated species **3a-H⁺** are shifted to lower field, where increased deshielding indicates the formation of a resonance stabilized cation. For instance, the methyl protons at position 5 are shifted from δ 3.26 (**3a**) to 3.73 (**3a-H⁺**). The protonation of **3a** to **3a-H⁺** also causes a significant change in the molecular geometry supported by the splitting the phenyl proton resonances. The resonances of 6-Ph (blue circles, Figure 7) split into a doublet and two triplets, which is indicative of the free rotation of the phenyl ring, whereas for 7-Ph (orange circles, Figure 7) split into five

broaden signals that appear between δ 6.59 and 7.72. This phenyl ring obviously is considerably restricted in its rotational freedom and therefore splits into five chemically inequivalent signals.

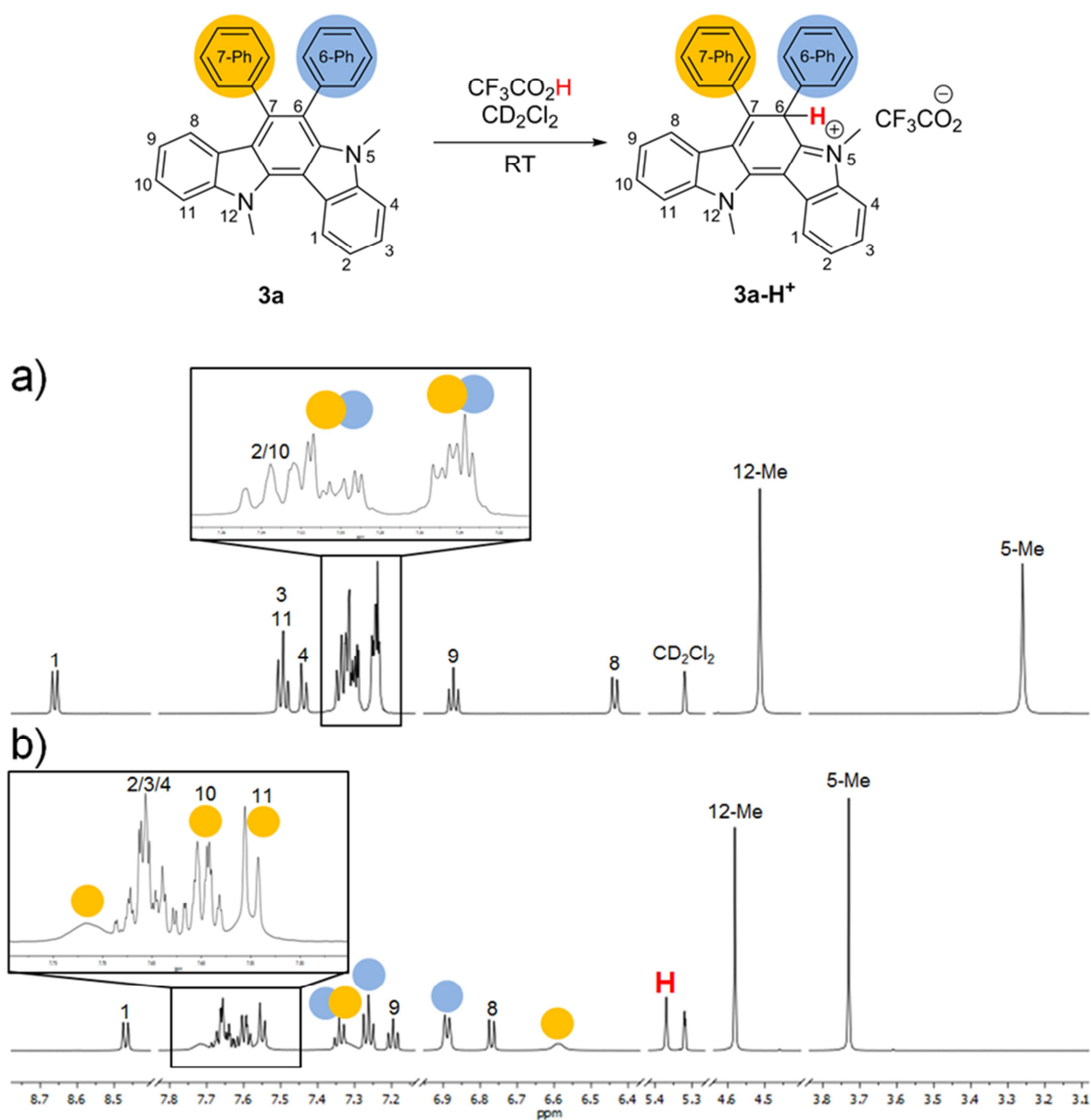


Figure 7. Partial ^1H NMR spectra (600 MHz, 293 K, CD_2Cl_2) of **3a** before (a) and after (b) the addition of 75 equiv of $\text{CF}_3\text{CO}_2\text{H}$.

2.4. Calculated electronic structure

Ground state geometries of all structures **3** and **3a-H⁺** were optimized using the Gaussian09 program package [37], the PBE0 hybrid-functional by Perdew, Burke and Ernzerhof [38] and the 6-311G(d,p) basis set [39]. The optimized geometries were confirmed as minima by analytical frequency analyses.

Excitation energies were calculated with TDDFT [40] methods implemented in the Gaussian09 program package [37], PBE0 [38], and the 6-311+G(d,p) basis set [39]. The polarizable continuum model (PCM) with dichloromethane as a solvent was applied for the calculations each [41]. The Mulliken population analysis was extracted from the Gaussian09 calculation outputs by the help of the Multiwfn software [42].

The site of protonation in structure **3a-H⁺**, experimentally assigned by NMR experiments, was further corroborated by DFT calculations also to gain a deeper insight into the observed acidochromism. All ground state geometries and excitation energies of the protonated species **3a-H⁺** and **3a** were calculated (for details, see Supp Inf). We hypothesized that in addition to the two indolyl nitrogen atoms, the three β -positions of the indoles are potential sites of protonation, i.e. a total of five different protonation sites have to be considered (Figure 8). The calculations on the different protonated species **3a-H⁺** reveal in agreement with the NMR spectroscopic study that protonation at position 6 forms the thermodynamically most stable cation (Table 4). Moreover, the position bearing the largest HOMO coefficient in the non-protonated compound **3a** was protonated (Table 4).

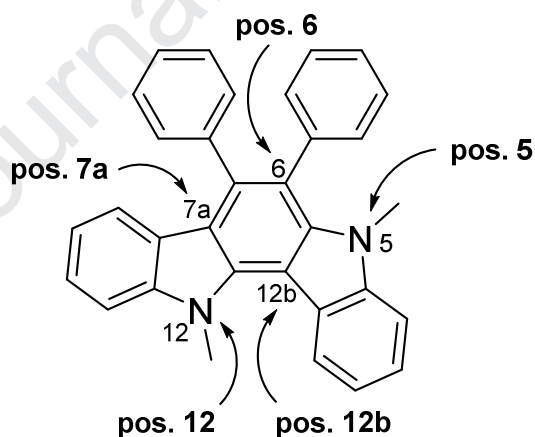


Figure 8. Potential protonation sites of **3a**.

Table 4. Relative free enthalpies (PBE0/6-311G(d,p) PCM CH₂Cl₂) of **3a-H⁺** protonated in all tested positions and the corresponding HOMO-coefficients of non-protonated **3a**.

position i	5	6	7a	12	12b
$\Delta\Delta G(\text{position } i \rightarrow \text{position } 6)$ [kcal/mol]	+8.81	0	+9.11	+6.00	+13.30
HOMO coefficients of 3a [%]	13.28	15.52	13.64	5.63	0.26

For the structure **3a-H⁺** with protonation at position 6 the UV/Vis spectrum was calculated on the TDDFT level of theory. The first states S₁, S₂, and S₃ nicely reproduce the experimentally observed absorption bands (Table 5). While the longest wavelength absorption band (S₁) can be described as a HOMO→LUMO transition (99%), the following bands consist of HOMO-2→LUMO (S₂, 94 %) and HOMO→LUMO+1 transitions (S₃, 84%) (for full details, see Supp Inf).

Table 5. Comparison of calculated UV/Vis-absorption of **3a-H⁺** (PBE0/6-311+G(d,p) PCM CH₂Cl₂), protonated in position 6, and experimental UV/Vis-absorption of **3a-H⁺**.

$\lambda_{max, exp}^{[a]}$ [nm]	$\lambda_{max, calc}^{[b]}$ [nm]	oscillator strength	FMO contribution
479	458	0.245	HOMO → LUMO (99 %)
367	360	0.162	HOMO-2 → LUMO (94 %) HOMO→LUMO+1 (3 %) HOMO-7 → LUMO (7 %)
297	288	0.544	HOMO-2 → LUMO (3 %) HOMO → LUMO+1 (84 %) HOMO-8 → LUMO (20 %) HOMO-5 → LUMO+1 (2 %) HOMO-1 → LUMO+1 (47 %)
277	256	0.387	HOMO-1 → LUMO+2 (9 %) HOMO → LUMO+2 (8 %) HOMO → LUMO+7 (3 %) HOMO → LUMO+8 (3 %)

[a] Recorded in CH₂Cl₂, $c(\mathbf{3a}) = 10^{-5}$ M, pH = 0.25, $T = 293$ K. [b] PBE0/6-311+G(d,p) with PCM (CH₂Cl₂).

Based upon the spectroscopic and computational studies supporting the protonation of structure **3a** at position 6 resonance structures of **3a-H⁺** can be assigned, suggesting that the formed chromophore is an apocyanine (Figure 9). An apocyanine is a rare type of cyanine where the two terminal nitrogen atoms are conjugatively linked without methine groups, i.e. only quaternary sp²-hybridized carbon centers [43]. This special topology rationalizes the bathochromic shift upon protonation (Figure 10). As seen from the NMR studies both phenyl groups are no longer parallel to each other and the substituent at position 7 planarizes with the indolocarbazole and participates in the conjugation with the apocyanine system.

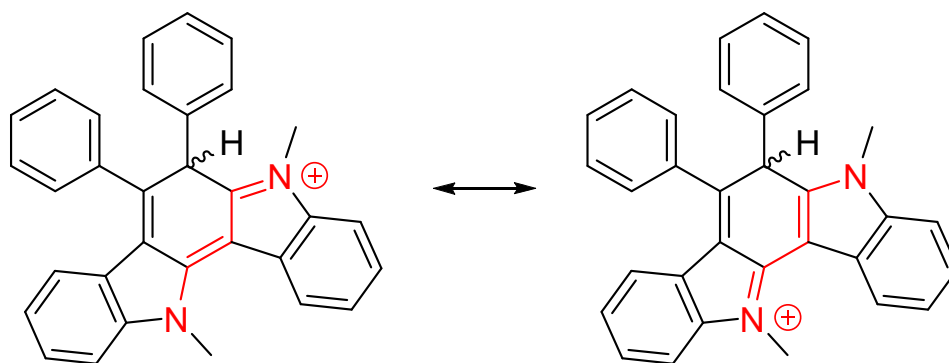


Figure 9. Resonance structures of a closed apocyanine system (red) arising from protonation of compound **3a**.

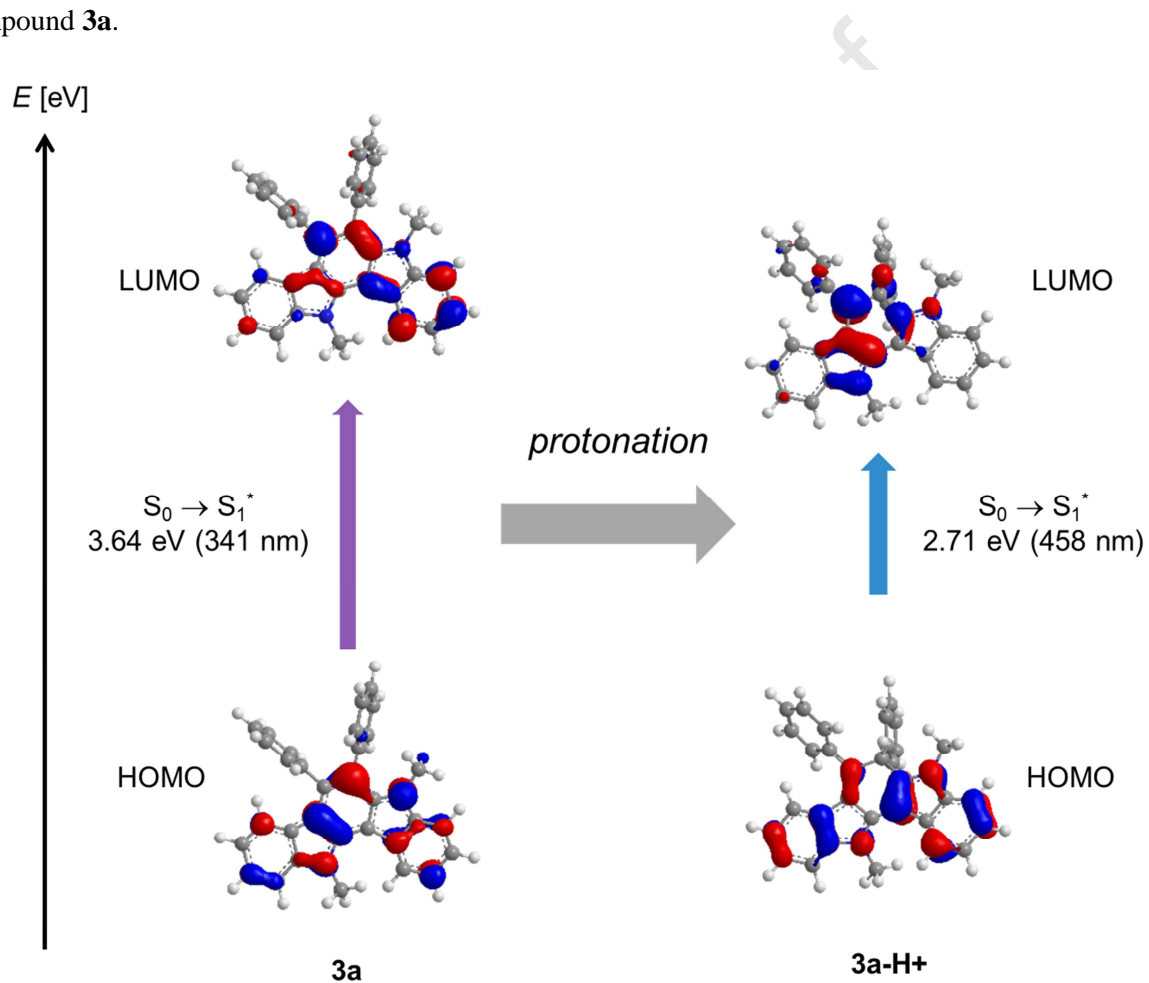


Figure 10. Jablonski diagram before (left) and after (right) protonation of **3a** and assignment of the FMO-transitions in the longest wavelength absorption bands (PBE0/6-311+G(d,p) PCM CH₂Cl₂, isosurface value at 0.04 a.u.).

3. Conclusion

In summary starting from indoles and alkynes we have disclosed an efficient and mild sequentially Pd(II)/Cu(II)-catalyzed pseudo-three-component domino reaction to give indolo[3,2-*a*]carbazoles even with strongly electron withdrawing groups. In addition, with a TIPS-protected alkyne as a substrate, it was possible to selectively obtain the mono-phenylated 7-phenylindolo[3,2-*a*]carbazole via in situ desilylation. The study of the electronic properties of the indolocarbazoles revealed in addition to the known fluorescence, to the best of our knowledge a hitherto unknown acidochromism of this class of compounds, indicating that the title compounds are reversibly pH-sensitive. The protonation site was unambiguously localized by NMR spectroscopy and confirmed by quantum chemical calculations. Protonation generates a rarely described intensively orange to red apocyanine system. Syntheses and applications of these novel electronically interesting apocyanine dyes are currently underway.

4. Experimental

4.1. General considerations

All reactions were carried out in flame-dried Schlenk tubes by using syringes under an oxygen atmosphere. Oxygen was used from a bottle of Air Liquide (ALPHAGAZ™ 1 O₂, 99.998 %). Indoles **1b** [44] and **1c** [32], as well as alkynes **2b** [45], **2c** [45], and **2d** [46] were synthesized according to literature procedures as indicated. Commercial grade reagents were purchased from Sigma Aldrich, Alfa Aesar, ABCR, Fluorochem and ACROS and used as supplied without further purification. Crude mixtures were adsorbed on Celite® 545 (0.02-0.20 mm) from Carl Roth GmbH Co.KG. The purification of products was performed on silica gel 60 M (0.04–0.063 mm) from Macherey–Nagel by using the flash technique under a pressure of 2 bar. For TLC silica gel coated aluminium plates (60, F₂₅₄) from Merck were employed. The spots were detected with UV light at 254 or 365 nm. ¹H, ¹³C, and DEPT NMR spectra were recorded at 293 K on 300 MHz (Bruker AVIII) or 600 MHz (BrukerAvance III-600) and the resonances of the residues of non-deuterated CD₂Cl₂ were locked as internal standards (CD₂Cl₂: ¹H δ = 5.32 ppm, ¹³C δ = 54.00 ppm). The multiplicities of signals are abbreviated as follows: s = singlet, d = doublet, t = triplet, dd = doublet of doublets, ddd = doublet of

doublets of doublets and $m =$ multiplet. The assignments of C_{quat} , CH, CH_2 and CH_3 nuclei are based on DEPT spectra. IR spectra were recorded on a Shimadzu IR Affinity-1 with ATR technique. The intensities of IR signals are abbreviated as s (strong), m (medium) and w (weak). EI mass spectra were recorded on Triple-Quadrupole mass spectrometer TSQ 7000 (Finnigan MAT). Absorption spectra were recorded in CH_2Cl_2 high performance liquid chromatography (HPLC) grade at 293 K on Perkin Elmer UV/VIS/ NIR Lambda 19 spectrometer. Emission spectra were recorded in CH_2Cl_2 HPLC grade at 293 K on a Perkin Elmer LS55 spectrometer. The melting points (uncorrected) were measured on a Büchi Melting Point B-540. The elemental analyses were carried out on a Perkin Elmer Series II Analyser 2400 at the Institute for Pharmaceutical and Medicinal Chemistry at Heinrich-Heine-University Düsseldorf.

4.2. General procedure (GP) for the domino synthesis of indolo[3,2-*a*]carbazoles **3**

Palladium(II)acetate (11.2 mg, 50.0 μmol , 10 mol%), copper(II)acetate monohydrate (24.9 mg, 125 μmol , 25 mol%), indole **1** (500 μmol , 1.00 equiv) and/or alkyne **2** (250 μmol , 0.50 equivs), if solid, were placed in a Schlenk tube, which was evacuated and flushed with oxygen three times. Then, indole **1** (500 μmol , 1.00 eq.) and/or alkyne **2** (250 μmol , 0.50 equivs), if present as a liquid, and DMSO (5 mL) were added. The reaction mixture was stirred until complete conversion (8 or 24 h, monitored by TLC, eluent: *n*-hexane/ethyl acetate) at 50 °C under an oxygen atmosphere. After cooling to room temp, the solvent was removed under reduced pressure, the product mixture adsorbed on Celite[®] and purified by column chromatography on silica gel (eluent: *n*-hexane/dichloromethane).

Table 6. Experimental details of the domino synthesis of indolo[3,2-*a*]carbazoles **3**.

entry	indole 1	alkyne 2	indolo[3,2- <i>a</i>]carbazoles 3 (yield)
1	65.6 mg (0.50 mmol) of 1-methylindole (1a)	44.6 mg (0.25 mmol) of tolane (2a)	78.7 mg (72%) of 3a
2	80.6 mg (0.50 mmol) of 5-methoxy-1-methylindole (1b)	44.6 mg (0.25 mmol) of 2a	90.8 mg (73%) of 3b
3	65.6 mg (0.50 mmol) of 1a	57.1 mg (0.25 mmol) of 1,2-bis(4-methoxyphenyl)ethyne (2b)	85.0 mg (68%) of 3c
4	80.6 mg (0.50 mmol) of 1b	57.1 mg (0.25 mmol) of 2b	83.3 mg (60%) of 3d
5	78.1 mg (0.50 mmol) of 1-methyl-indole-5-carbonitrile (2c)	44.6 mg (0.25 mmol) of 2a	70.0 mg (58%) of 3e
6	65.6 mg (0.50 mmol) of 1a	57.1 mg (0.25 mmol) of 4,4'-(ethyne-1,2-diyl)dibenzonitrile (2c)	62.5 mg (51%) of 3f

7	65.6 mg (0.50 mmol) of 1a	129 mg (0.50 mmol) of triisopropyl(phenylethynyl)silane (2d)	61.5 mg (68%) of 3g
---	----------------------------------	---	----------------------------

4.2.1. 5,12-Dimethyl-6,7-diphenyl-5,12-dihydroindolo[3,2-*a*]carbazole (**3a**)

According to the GP compound **3a** (78.7 mg, 72%) was obtained as a colorless solid. Mp 141–142 °C (lit. 140–142 °C [26]). ¹H NMR (CD₂Cl₂, 600 MHz): δ 3.14 (s, 3 H), 4.39 (s, 3 H), 6.32 (d, *J* = 7.9 Hz, 1 H), 6.76 (t, *J* = 7.5 Hz, 1 H), 7.10–7.15 (m, 5 H), 7.15–7.25 (m, 7 H), 7.32 (d, *J* = 8.1 Hz, 1 H), 7.37 (t, *J* = 7.6 Hz, 2 H), 8.54 (d, *J* = 8.1 Hz, 1 H). ¹³C NMR (CD₂Cl₂, 151 MHz): δ 33.3 (CH₃), 36.0 (CH₃), 107.6 (C_{quat}), 109.5 (CH), 109.7 (CH), 115.5 (C_{quat}), 118.9 (C_{quat}), 119.7 (2xCH), 121.3 (C_{quat}), 121.5 (CH), 123.2 (CH), 124.3 (CH), 124.9 (CH), 124.9 (C_{quat}), 127.2 (CH), 127.2 (CH), 127.8 (CH), 128.4 (CH), 130.9 (CH), 133.0 (CH), 136.1 (C_{quat}), 137.4 (C_{quat}), 139.4 (C_{quat}), 139.8 (C_{quat}), 140.9 (C_{quat}), 142.4 (C_{quat}), 142.9 (C_{quat}). EI-MS (70 eV, *m/z* (%)): 436 ([M]⁺, 100), 421 ([M-CH₃]⁺, 15), 406 ([M-2x(CH₃)]⁺, 9), 203 (16), 202 (17), 201 (11), 196 (11). IR (ATR): $\tilde{\nu}$ [cm⁻¹] 3044 (w), 1580 (m), 1570 (m), 1558 (m), 1441 (m), 1329 (m), 1315 (m), 1256 (m), 1024 (m), 968 (m), 918 (m), 768 (m), 752 (m), 729 (s), 718 (s). Anal. calcd. for C₃₂H₂₄N₂ (436.6): C 88.04, H 5.54, N 6.42; Found: C 88.11, H 5.55, N 6.20.

4.2.2. 2,9-Dimethoxy-5,12-dimethyl-6,7-diphenyl-5,12-dihydroindolo[3,2-*a*]carbazole (**3b**)

According to the GP compound **3b** (90.8 mg, 73%) was obtained as a colorless solid. Mp 197–198 °C (lit. 160–165 °C [26]). ¹H NMR (CD₂Cl₂, 600 MHz): δ 3.19 (s, 3 H), 3.88 (s, 3 H), 3.94 (s, 3 H), 4.41 (s, 3 H), 6.29 (d, *J* = 8.2 Hz, 1 H), 6.48 (dd, *J* = 8.6, 2.1 Hz, 1 H), 6.86 (s, 1 H), 6.91–6.94 (m, 1 H), 6.95 (d, *J* = 2.1 Hz, 1 H), 7.20–7.25 (m, 5 H), 7.26–7.33 (m, 5 H), 8.47 (d, *J* = 8.8 Hz, 1 H). ¹³C NMR (CD₂Cl₂, 151 MHz): δ 33.4 (CH₃), 35.9 (CH₃), 56.1 (CH₃), 56.1 (CH₃), 93.7 (CH), 94.2 (CH), 107.6 (CH), 107.9 (C_{quat}), 108.1 (CH), 115.1 (C_{quat}), 115.8 (C_{quat}), 118.8 (C_{quat}), 119.0 (C_{quat}), 122.1 (CH), 123.9 (CH), 125.4 (CH), 127.1 (CH), 127.7 (CH), 128.4 (CH), 131.1 (CH), 132.9 (CH), 134.1 (C_{quat}), 136.7 (C_{quat}), 139.2 (C_{quat}), 139.6 (C_{quat}), 141.0 (C_{quat}), 143.9 (C_{quat}), 144.2 (C_{quat}), 158.4 (C_{quat}), 158.6 (C_{quat}). EI-MS (70 eV, *m/z* (%)): 497 ([MH]⁺, 100), 482 ([M-CH₃]⁺, 14), 453 (12), 438 (11), 395 (11), 248 (22), 196 (11), 189 (12), 97 (13), 85 (10), 83 (12), 71 (13), 69 (12), 57 (18), 55 (12). IR (ATR): $\tilde{\nu}$ [cm⁻¹] 3019 (w), 1585 (w), 1393 (m), 1219 (m), 1086 (s), 1032 (m), 982 (m), 802 (s), 706 (s). Anal. calcd. for C₃₄H₂₈N₂O₂ (496.6): C 82.23, H 5.68, N 5.64; Found: C 81.97, H 5.53, N 5.62.

4.2.3. 6,7-Bis(4-methoxyphenyl)-5,12-dimethyl-5,12-dihydroindolo[3,2-*a*]carbazole (3c)

According to the GP compound **3c** (85.0 mg, 68%) was obtained as a colorless solid. Mp 334–335 °C (dec.). ¹H NMR (CD₂Cl₂, 300 MHz): δ 3.28 (s, 3 H), 3.80 (s, 3 H), 3.84 (s, 3 H), 4.51 (s, 3 H), 6.53 (d, $J = 7.9$ Hz, 1 H), 6.76–6.81 (m, 2 H), 6.84–6.92 (m, 2 H), 7.11–7.15 (m, 2 H), 7.16–7.20 (m, 2 H), 7.29–7.36 (m, 2 H), 7.42–7.51 (m, 3 H), 8.64 (d, $J = 8.1$ Hz, 1 H). ¹³C NMR (CD₂Cl₂, 75 MHz): δ 33.4 (CH₃), 36.1 (CH₃), 55.8 (CH₃), 55.8 (CH₃), 107.7 (C_{quat.}), 109.5 (CH), 109.8 (CH), 113.4 (CH), 114.0 (CH), 116.1 (C_{quat.}), 119.2 (C_{quat.}), 119.7 (CH), 119.8 (CH), 121.5 (C_{quat.}), 121.7 (CH), 123.2 (CH), 124.3 (CH), 124.9 (CH), 125.3 (C_{quat.}), 131.8 (C_{quat.}), 132.0 (CH), 133.4 (C_{quat.}), 133.9 (CH), 136.4 (C_{quat.}), 137.5 (C_{quat.}), 140.4 (C_{quat.}), 142.6 (C_{quat.}), 143.1 (C_{quat.}), 159.1 (C_{quat.}), 159.1 (C_{quat.}). EI-MS (70 eV, m/z (%)): 496 ([M]⁺, 100), 196 (12), 189 (12). IR (ATR): $\tilde{\nu}$ [cm⁻¹] 2951 (w), 2932 (w), 2900 (w), 1518 (m), 1449 (m), 1315 (m), 1282 (m), 1240 (s), 1177 (m), 1030 (m), 826 (m), 781 (m), 739 (s). Anal. calcd. for C₃₄H₂₈N₂O₂ (496.6): C 82.23, H 5.68, N 5.64; Found: C 82.29, H 5.55, N 5.59.

4.2.4. 2,9-Dimethoxy-6,7-bis(4-methoxyphenyl)-5,12-dimethyl-5,12-dihydroindolo[3,2-*a*]carbazole (3d)

According to the GP compound **3d** (83.3 mg, 60%) was obtained as a colorless solid. Mp 238–239 °C. ¹H NMR (CD₂Cl₂, 300 MHz): δ 3.23 (s, 3 H), 3.50 (s, 3 H), 3.78 (s, 3 H), 3.79 (s, 3 H), 3.97 (s, 3 H), 4.44 (s, 3 H), 5.92 (d, $J = 2.6$ Hz, 1 H), 6.77 (d, $J = 8.6$ Hz, 2 H), 6.86 (d, $J = 8.6$ Hz, 2 H), 6.92 (dd, $J = 8.8, 2.6$ Hz, 1 H), 7.08–7.20 (m, 5 H), 7.34 (t, $J = 8.7$ Hz, 2 H), 8.11 (d, $J = 2.4$ Hz, 1 H). ¹³C NMR (CD₂Cl₂, 75 MHz): δ 33.4 (CH₃), 36.2 (CH₃), 55.7 (CH₃), 55.9 (CH₃), 55.9 (CH₃), 56.8 (CH₃), 104.9 (CH), 107.4 (CH), 107.7, 110.0 (CH), 110.2 (CH), 112.9 (CH), 113.3 (CH), 113.4 (CH), 114.0 (CH), 118.9 (C_{quat.}), 121.8 (C_{quat.}), 125.9 (C_{quat.}), 131.7 (C_{quat.}), 132.2 (CH), 133.4 (C_{quat.}), 133.9 (CH), 136.4 (C_{quat.}), 137.8 (C_{quat.}), 138.1 (C_{quat.}), 138.3 (C_{quat.}), 141.0 (C_{quat.}), 154.3 (C_{quat.}), 154.4 (C_{quat.}), 159.1 (C_{quat.}), 159.2 (C_{quat.}). EI-MS (70 eV, m/z (%)): 556 ([M]⁺, 100), 541 ([M-CH₃]⁺, 21), 278 (15), 247 (9), 196 (8). IR (ATR): $\tilde{\nu}$ [cm⁻¹] 3063 (w), 2830 (w), 2359 (w), 2342 (w), 1518 (m), 1508 (m), 1487 (m), 1448 (m), 1375 (w), 1302 (m), 1244 (s), 1233 (s), 1213 (s), 1175 (s), 1150 (s), 1105 (m), 1030 (s), 978 (m), 935 (m), 874 (m), 849 (m), 831 (m), 808 (m), 781 (s), 756 (m), 729 (m), 687 (m). Anal. calcd. for C₃₆H₃₂N₂O₄ (556.7): C 77.68, H 5.79, N 5.03. Found: C 77.39, H 5.87, N 4.96.

4.2.5. 5,12-Dimethyl-6,7-diphenyl-5,12-dihydroindolo[3,2-*a*]carbazole-2,9-dicarbonitrile (3e)

According to the GP compound **3e** (70.0 mg, 58%) was obtained as a colorless solid. Mp 381–383 °C (dec.). ¹H NMR (CD₂Cl₂, 300 MHz): δ 3.31 (s, 3 H), 4.55 (s, 3 H), 6.64–6.67 (m, 1 H), 7.19–7.23 (m, 2 H), 7.25–7.30 (m, 5 H), 7.34–7.41 (m, 3 H), 7.51 (d, *J* = 8.6 Hz, 1 H), 7.55–7.59 (m, 1 H), 7.61 (dd, *J* = 8.5, 1.5 Hz, 1 H), 7.75 (dd, *J* = 8.6, 1.5 Hz, 1 H), 8.93 (d, *J* = 1.2 Hz, 1 H). ¹³C NMR (CD₂Cl₂, 75 MHz): δ 33.9 (CH₃), 36.2 (CH₃), 103.1 (C_{quat}), 103.1 (C_{quat}), 107.4 (C_{quat}), 110.4 (CH), 110.8 (CH), 116.0 (C_{quat}), 120.7 (C_{quat}), 120.9 (C_{quat}), 121.1 (C_{quat}), 121.3 (C_{quat}), 124.9 (C_{quat}), 126.6 (CH), 127.9 (CH), 128.0 (CH), 128.1 (CH), 128.1 (CH), 128.2 (CH), 128.5 (CH), 129.0 (CH), 130.6 (CH), 132.8 (CH), 137.8 (C_{quat}), 138.0 (C_{quat}), 138.3 (C_{quat}), 139.7 (C_{quat}), 141.2 (C_{quat}), 144.2 (C_{quat}), 144.3 (C_{quat}). EI-MS (70 eV, *m/z* (%)): 486 ([M]⁺, 100), 471 ([M-CH₃]⁺, 11), 236 (15), 228 (11), 227 (12), 214 (10). IR (ATR): $\tilde{\nu}$ [cm⁻¹] 3065 (w), 2916 (w), 2802 (w), 2214 (m), 1576 (m), 1489 (m), 1441 (m), 1300 (m), 1261 (m), 976 (w), 935 (w), 820 (s), 704 (s). Anal. calcd. for C₃₄H₂₂N₄ (486.6): C 83.93, H 4.56, N 11.51; Found: C 83.85, 4.40, N 11.34.

4.2.6. 4,4'-(5,12-Dimethyl-5,12-dihydroindolo[3,2-*a*]carbazole-6,7-diyl)dibenzonitrile (3f)

According to the GP compound **3f** (62.5 mg, 51%) was obtained as a colorless solid. Mp 323–324 °C. ¹H NMR (CD₂Cl₂, 300 MHz): δ 3.27 (s, 3 H), 4.52 (s, 3 H), 6.46 (d, *J* = 7.9 Hz, 1 H), 6.92 (ddd, *J* = 8.1, 7.1, 1.0 Hz, 1 H), 7.31–7.41 (m, 6 H), 7.45–7.56 (m, 5 H), 7.62 (d, *J* = 8.3 Hz, 2 H), 8.67 (d, *J* = 8.1 Hz, 1 H). ¹³C NMR (CD₂Cl₂, 75 MHz): δ 34.0 (CH₃), 36.1 (CH₃), 108.6 (C_{quat}), 109.9 (CH), 110.1 (CH), 111.7 (C_{quat}), 111.9 (C_{quat}), 115.0 (C_{quat}), 116.8 (C_{quat}), 119.2 (C_{quat}), 119.4 (C_{quat}), 120.3 (CH), 120.3 (CH), 121.2 (CH), 123.5 (CH), 124.3 (C_{quat}), 125.0 (CH), 125.6 (CH), 131.9 (CH), 132.0 (CH), 132.7 (CH), 133.6 (CH), 133.9 (C_{quat}), 138.2, (C_{quat}) 139.4 (C_{quat}), 142.7 (C_{quat}), 143.1 (C_{quat}), 144.4 (C_{quat}), 145.5 (C_{quat}). EI-MS (70 eV, *m/z* (%)): 486 ([M]⁺, 100), 471 ([M-CH₃]⁺, 14), 236 (15). IR (ATR): $\tilde{\nu}$ [cm⁻¹] 2990 (w), 2899 (w), 2365 (w), 2361 (w), 2231 (w), 1589 (m), 1585 (m), 1474 (m), 1389 (m), 1319 (m), 1258 (m), 1179 (m), 1092 (m), 1016 (m), 995 (m), 974 (m), 864 (m), 781 (m), 746 (m), 731 (s), 689 (m). Anal. calcd. for C₃₄H₂₂N₄ (486.6): C 83.93, H 4.56, N 11.51. Found: C 83.98, H 4.52, N 11.53.

4.2.7. 5,12-Dimethyl-7-phenyl-5,12-dihydroindolo[3,2-*a*]carbazol (**3g**)

According to the GP compound **3g** (61.5 mg, 68%) was obtained as a colorless solid. Mp 192–194 °C. ¹H NMR (CD₂Cl₂, 300 MHz): δ 3.94 (s, 3H), 4.53 (s, 3 H), 6.98 (ddd, *J* = 8.0, 7.0, 1.1 Hz, 1 H), 7.19 (s, 1 H), 7.26 (d, *J* = 7.9 Hz, 1 H), 7.29–7.40 (m, 2 H), 7.48–7.61 (m, 6 H), 7.66–7.70 (m, 2 H), 8.63 (d, *J* = 8.2 Hz, 1 H). ¹³C NMR (CD₂Cl₂, 75 MHz): δ 30.2 (CH₃), 35.6, (CH₃) 104.1 (C_{quat}), 104.1 (C_{quat}), 106.6 (C_{quat}), 109.4 (CH), 109.5 (CH), 119.6 (CH), 119.7 (CH), 121.6 (CH), 121.7 (C_{quat}), 123.4 (CH), 124.3 (CH), 124.6 (C_{quat}), 124.9 (CH), 125.6 (C_{quat}), 128.2 (CH), 129.0 (CH), 130.1 (CH), 138.7 (C_{quat}), 141.5 (C_{quat}), 142.0 (C_{quat}), 142.2 (C_{quat}), 142.8 (C_{quat}). EI-MS (70 eV, *m/z* (%)): 360 ([M]⁺, 100), 345 ([M-CH₃]⁺, 20), 330 ([M-2x(CH₃)]⁺, 10), 180 (12), 172 (32), 165 (18). IR (ATR): $\tilde{\nu}$ [cm⁻¹] 2984 (w), 2970 (w), 2901 (w), 1591 (w), 1558 (m), 1479 (m), 1448 (m), 1435 (m), 1408 (m), 1348 (m), 1317 (s), 1250 (m), 1231 (m), 1190 (m), 1119 (m), 1057 (m), 1024 (m), 972 (m), 960 (m), 921 (w), 885 (m), 841 (m), 820 (m), 773 (m), 756 (m), 742 (s), 727 (s), 708 (s), 696 (s), 650 (m). Anal. calcd. for C₂₆H₂₀N₂ (360.5): C 86.64, H 5.59, N 7.77. Found: C 86.93, H 5.74, N 7.87.

5. Acknowledgements

We cordially thank the Fonds der Chemischen Industrie and Deutsche Forschungsgemeinschaft (Mu 1088/9-1) for the financial support. And we are grateful to M. Sc. Tobias Wilcke for taking the photographs. Computational support and infrastructure was provided by the “Centre for Information and Media Technology” (ZIM) at the University of Düsseldorf (Germany).

6. References

- [1] a) Levi L, Müller TJJ. Multicomponent Syntheses of Functional Chromophores. *Chem Soc Rev* 2016;45:2825-46; b) Levi L, Müller TJJ. Multicomponent Syntheses of Fluorophores Initiated by Metal Catalysis. *Eur J Org Chem* 2016;2016:2902-18; c) Müller TJJ, Bunz UHF, eds., *Functional Organic Materials*. Weinheim: Wiley-VHC; 2007.
- [2] a) Zhu J, Wang Q, Wang M, *Multicomponent Reactions in Organic Synthesis* Weinheim: Wiley-VHC; 2014; b) Müller T, *Multicomponent Reactions 1. General Discussion and Reactions Involving a Carbonyl Compound as Electrophilic Component*. Stuttgart: Georg Thieme; 2014; c) D'Souza DM, Müller TJJ. Multi-component Syntheses of Heterocycles by Transition-Metal Catalysis. *Chem Soc Rev* 2007;36:1095-108; d) Dömling A, Ugi I. *Multicomponent Reactions with Isocyanides*. *Angew Chem Int Ed* 2000;39:3168-210.
- [3] a) D'Souza DM, Kiel A, Herten D-P, Rominger F, Müller TJJ. Synthesis, Structure and Emission Properties of Spirocyclic Benzofuranones and Dihydroindolones: A Domino Insertion–Coupling–Isomerization–Diels–Alder Approach to Rigid Fluorophores. *Chem Eur J*

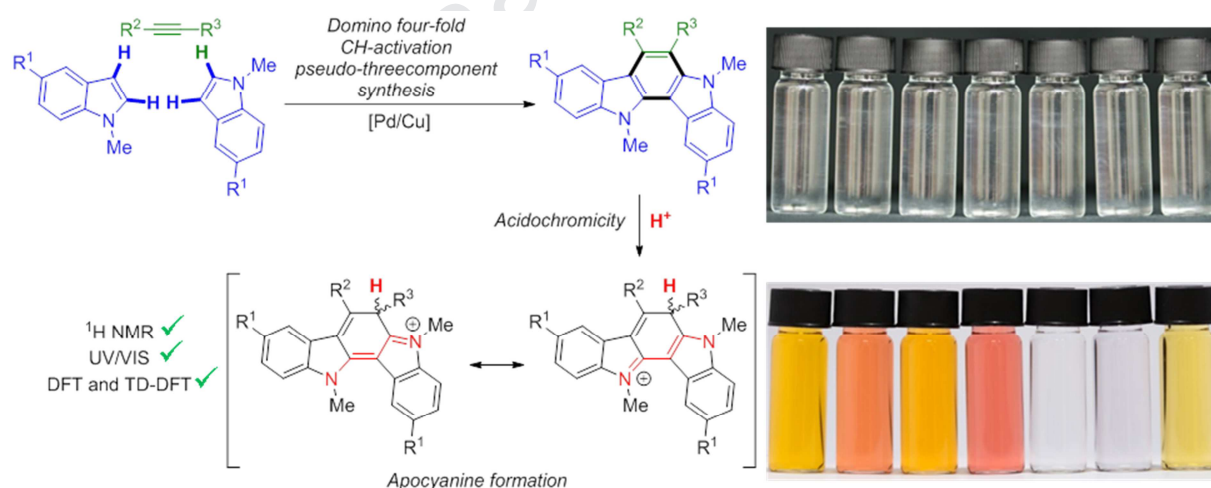
- 2008;14:529-47; b) D'Souza DM, Rominger F, Müller TJJ. A Domino Sequence Consisting of Insertion, Coupling, Isomerization, and Diels–Alder Steps Yields Highly Fluorescent Spirocycles. *Angew Chem Int Ed* 2005;44:153-8.
- [4] a) Park J-S, Chae H, Chung HK, Lee SI. Thin Film Encapsulation for Flexible AM-OLED: a Review. *Semicond Sci Technol* 2011;26:034001; b) Thejo Kalyani N, Dhoble SJ. Organic Light Emitting Diodes: Energy Saving Lighting Technology—A Review. *Renew Sustain Energy Rev* 2012;16:2696-723.
- [5] a) Shalini S, Balasundaraprabhu R, Kumar TS, Prabavathy N, Senthilarasu S, Prasanna S. Status and Outlook of Sensitizers/Dyes Used in Dye Sensitized Solar Cells (DSSC): A Review. *Int J Energy Res* 2016;40:1303-20; b) Sugathan V, John E, Sudhakar K. Recent Improvements in Dye Sensitized Solar Cells: A Review. *Renew Sustain Energy Rev* 2015;52:54-64; c) Richhariya G, Kumar A, Tekasakul P, Gupta B. Natural Dyes for Dye Sensitized Solar Cell: A Review. *Renew Sustain Energy Rev* 2017;69:705-18.
- [6] a) Lizin S, Van Passel S, De Schepper E, Maes W, Lutsen L, Manca J, Vanderzande D. Life Cycle Analyses of Organic Photovoltaics: A Review. *Energy Environ Sci* 2013;6:3136-49; b) Yu J, Zheng Y, Huang J. Towards High Performance Organic Photovoltaic Cells: A Review of Recent Development in Organic Photovoltaics. *Polymers* 2014;6; c) Su Y-W, Lan S-C, Wei K-H. Organic Photovoltaics. *Mater Today* 2012;15:554-62.
- [7] a) Chen C-T, Wagner H, Still WC. Fluorescent, Sequence-Selective Peptide Detection by Synthetic Small Molecules. *Science* 1998;279:851; b) Nilsson D, Kugler T, Svensson P-O, Berggren M. An All-Organic Sensor–Transistor Based on a Novel Electrochemical Transducer Concept Printed Electrochemical Sensors on Paper. *Sens Actuator B Chem* 2002;86:193-7; c) Grunwald C, Schulze K, Reichel A, Weiss VU, Blaas D, Piehler J, Wiesmüller K-H, Tampé R. In Situ Assembly of Macromolecular Complexes Triggered by Light. *Proc Natl Acad Sci* 2010;107:6146; d) McQuade DT, Pullen AE, Swager TM. Conjugated Polymer-Based Chemical Sensors. *Chem Rev* 2000;100:2537-74.
- [8] a) Irie M, Fukaminato T, Matsuda K, Kobatake S. Photochromism of Diarylethene Molecules and Crystals: Memories, Switches, and Actuators. *Chem Rev* 2014;114:12174-277; b) Klajn R. Spiropyran-based Dynamic Materials. *Chem Soc Rev* 2014;43:148-84.
- [9] Seeboth A, Löttsch D, Ruhmann R, Muehling O. Thermochromic Polymers—Function by Design. *Chem Rev* 2014;114:3037-68.
- [10] Yang P, Sun P, Mai W. Electrochromic Energy Storage Devices. *Mater Today* 2016;19:394-402.
- [11] a) Jaffe A, Lin Y, Mao WL, Karunadasa HI. Pressure-Induced Conductivity and Yellow-to-Black Piezochromism in a Layered Cu–Cl Hybrid Perovskite. *J Am Chem Soc* 2015;137:1673-8; b) Sui Q, Ren X-T, Dai Y-X, Wang K, Li W-T, Gong T, Fang J-J, Zou B, Gao E-Q, Wang L. Piezochromism and Hydrochromism through Electron Transfer: New Stories for Viologen Materials. *Chem Sci* 2017;8:2758-68.
- [12] a) Machado VG, Stock RI, Reichardt C. Pyridinium N-Phenolate Betaine Dyes. *Chem Rev* 2014;114:10429-75; b) Reichardt C. Solvatochromic Dyes as Solvent Polarity Indicators. *Chem Rev* 1994;94:2319-58.
- [13] a) Ghazvini Zadeh EH, Tang S, Woodward AW, Liu T, Bondar MV, Belfield KD. Chromophoric Materials Derived from a Natural Azulene: Syntheses, Halochromism and One-Photon and Two-Photon Microlithography. *J Mater Chem C* 2015;3:8495-503; b) Sachdeva T, Milton MD. Logic Gate based Novel Phenothiazine-pyridylhydrazones: Halochromism in Solid and Solution State. *Dyes Pigment* 2019;164:305-18; c) Stolar M, Baumgartner T. Synthesis and Unexpected Halochromism of Carbazole-functionalized Dithienophospholes. *New J Chem* 2012;36:1153-60; d) Singh P, Baheti A, Thomas KRJ. Synthesis and Optical Properties of Acidochromic Amine-Substituted Benzo[a]phenazines. *J Org Chem* 2011;76:6134-45.
- [14] Speight JG, Lange's Handbook of Chemistry. New York: McGraw-Hill Education; 2005.
- [15] a) Garcia-Amorós J, Swaminathan S, Raymo FM. Saving Paper with Switchable Ink. *Dyes Pigment* 2014;106:71-3; b) Sheng L, Li M, Zhu S, Li H, Xi G, Li Y-G, Wang Y, Li Q, Liang S, Zhong K, Zhang SX-A. Hydrochromic Molecular Switches for Water-jet Rewritable Paper. *Nat Commun* 2014;5:3044.
- [16] Lakowicz JR, Principles of Fluorescence Spectroscopy. 3 ed. New York, NY: Springer; 2006.

- [17] Janosik T, Rannug A, Rannug U, Wahlström N, Slätt J, Bergman J. Chemistry and Properties of Indolocarbazoles. *Chem Rev* 2018;118:9058-128.
- [18] a) Mann FG, Willcox TJ. 305. The Synthesis of Indolo(2' : 3'-1 : 2)- and Indolo(3' : 2'-1 : 2)-carbazole. *J Chem Soc* 1958:1525-9; b) Brunton RJ, Drayson FK, Plant SGP, Tomlinson ML. 933. Experiments on the Preparation of Indolocarbazoles. Part IX. The Preparation of 9-Methylindolo(2' : 3'-1 : 2)carbazole. *J Chem Soc* 1956:4783-5.
- [19] Kase H, Iwahashi K, Nakanishi S, Matsuda Y, Yamada K, Takahashi M, Murakata C, Sato A, Kaneko M. K-252 Compounds, Novel and Potent Inhibitors of Protein Kinase C and Cyclic Nucleotide-dependent Protein Kinases. *Biochem Biophys Res Commun* 1987;142:436-40.
- [20] Furusaki A, Hashiba N, Matsumoto T, Hirano A, Iwai Y, Mura S. The Crystal and Molecular Structure of Staurosporine, a New Alkaloid from a *Streptomyces* Strain. *Bull Chem Soc Jpn* 1982;55:3681-5.
- [21] a) Civenni G, Longoni N, Costales P, Dallavalle C, García Inclán C, Albino D, Nuñez LE, Morís F, Carbone GM, Catapano CV. EC-70124, a Novel Glycosylated Indolocarbazole Multikinase Inhibitor, Reverts Tumorigenic and Stem Cell Properties in Prostate Cancer by Inhibiting STAT3 and NF- κ B. *Mol Cancer Ther* 2016;15:806; b) Bailly C, Riou J-F, Colson P, Houssier C, Rodrigues-Pereira E, Prudhomme M. DNA Cleavage by Topoisomerase I in the Presence of Indolocarbazole Derivatives of Rebeccamycin. *Biochemistry* 1997;36:3917-29; c) Yoshinari T, Ohkubo M, Fukasawa K, Egashira S-i, Hara Y, Matsumoto M, Nakai K, Arakawa H, Morishima H, Nishimura S. Mode of Action of a New Indolocarbazole Anticancer Agent, J-107088, Targeting Topoisomerase I. *Cancer Res* 1999;59:4271; d) Salas JA, Méndez C. Indolocarbazole Antitumor Compounds by Combinatorial Biosynthesis. *Curr Opin Chem Biol* 2009;13:152-60; e) Bailly C, Qu X, Chaires JB, Colson P, Houssier C, Ohkubo M, Nishimura S, Yoshinari T. Substitution at the F-Ring N-Imide of the Indolocarbazole Antitumor Drug NB-506 Increases the Cytotoxicity, DNA Binding, and Topoisomerase I Inhibition Activities. *J Med Chem* 1999;42:2927-35.
- [22] a) Brown A, Mullen KM, Ryu J, Chmielewski MJ, Santos SM, Felix V, Thompson AL, Warren JE, Pascu SI, Beer PD. Interlocked Host Anion Recognition by an Indolocarbazole-Containing [2]Rotaxane. *J Am Chem Soc* 2009;131:4937-52; b) Park JH, Lee HS, Park S, Min S-W, Yi Y, Cho C-G, Han J, Kim TW, Im S. Photo-Stable Organic Thin-Film Transistor Utilizing a New Indolocarbazole Derivative for Image Pixel and Logic Applications. *Adv Funct Mater* 2014;24:1109-16; c) Mai R, Wu X, Jiang Y, Meng Y, Liu B, Hu X, Roncali J, Zhou G, Liu J-M, Kempa K, Gao J. An Efficient Multi-functional Material based on Polyether-substituted Indolocarbazole for Perovskite Solar Cells and Solution-processed non-Doped OLEDs. *J Mater Chem A* 2019;7:1539-47; d) Lai C-C, Huang M-J, Chou H-H, Liao C-Y, Rajamalli P, Cheng C-H. m-Indolocarbazole Derivative as a Universal Host Material for RGB and White Phosphorescent OLEDs. *Adv Funct Mater* 2015;25:5548-56; e) Zhang D, Song X, Cai M, Kaji H, Duan L. Versatile Indolocarbazole-Isomer Derivatives as Highly Emissive Emitters and Ideal Hosts for Thermally Activated Delayed Fluorescent OLEDs with Alleviated Efficiency Roll-Off. *Adv Mater* 2018;30:1705406; f) Jiang H, Hu P, Ye J, Chaturvedi A, Zhang KK, Li Y, Long Y, Fichou D, Kloc C, Hu W. From Linear to Angular Isomers: Achieving Tunable Charge Transport in Single-Crystal Indolocarbazoles Through Delicate Synergetic CH/NH $\cdots\pi$ Interactions. *Angew Chem Int Ed* 2018;57:8875-80; g) Chen G, Sun S, Yang Y, Lan L, Ying L, Yang W, Zhang B, Cao Y. A Solution-processed and low Threshold voltage Voltage p-type Small Molecule based on Indolocarbazole- and Benzothiophene-fused Rings. *Dyes Pigment* 2017;144:32-40.
- [23] Kotha S, Saifuddin M, Aswar VR. A Diversity-oriented Approach to Indolocarbazoles via Fischer indolization and Olefin Metathesis: Total Synthesis of Tjipanazole D and I. *Org Biomol Chem* 2016;14:9868-73.
- [24] Shi Z, Ding S, Cui Y, Jiao N. A Palladium-Catalyzed Oxidative Cycloaromatization of Biaryls with Alkynes Using Molecular Oxygen as the Oxidant. *Angew Chem Int Ed* 2009;48:7895-8.
- [25] a) An Y-L, Yang Z-H, Zhang H-H, Zhao S-Y. Palladium-Catalyzed Tandem Regioselective Oxidative Coupling from Indoles and Maleimides: One-Pot Synthesis of Indolopyrrolo-carbazoles and Related Indolylmaleimides. *Org Lett* 2016;18:152-5; b) Nair V, Nandialath V, Abhilash KG, Suresh E. An Efficient Synthesis of Indolo[3,2-a]carbazoles via

- the Novel Acid Catalyzed Reaction of Indoles and Diaryl-1,2-diones. *Org Biomol Chem* 2008;6:1738-42.
- [26] Kumar KS, Meesa SR, Naikawadi PK. Palladium-Catalyzed [2 + 2 + 2] Annulation via Transformations of Multiple C–H Bonds: One-Pot Synthesis of Diverse Indolo[3,2-*a*]carbazoles. *Org Lett* 2018;20:6079-83.
- [27] a) Niesobski P, Klukas F, Berens H, Makhloufi G, Janiak C, Müller TJJ. De Novo Ring-Forming Consecutive Four-Component Syntheses of 4-Pyrazolyl-1,2,3-triazoles from (Triisopropylsilyl)butadiyne as a C4 Building Block. *J Org Chem* 2018;83:4851-8; b) Merkul E, Klukas F, Dorsch D, Grädler U, Greiner HE, Müller TJJ. Rapid Preparation of Triazolyl Substituted NH-Heterocyclic Kinase Inhibitors via One-pot Sonogashira Coupling–TMS-Deprotection–CuAAC Sequence. *Org Biomol Chem* 2011;9:5129-36; c) Merkul E, Urselmann D, Müller TJJ. Consecutive One-Pot Sonogashira–Glaser Coupling Sequence – Direct Preparation of Symmetrical Dienes by Sequential Pd/Cu Catalysis. *Eur J Org Chem* 2011;2011:238-42; d) Niesobski P, Santana Martínez I, Kustos S, Müller TJJ. Sequentially Pd/Cu-catalyzed Alkynylation-Oxidation Synthesis of 1,2-Diketones and Consecutive One-Pot Generation of Quinoxalines. *Eur J Org Chem* 2019;submitted for publication.
- [28] Lessing T, Müller TJJ. Sequentially Palladium-Catalyzed Processes in One-Pot Syntheses of Heterocycles. *Appl Sci* 2015;5.
- [29] Cinar R, Nordmann J, Dirksen E, Müller TJJ. Domino Synthesis of Protochromic “ON–OFF–ON” Luminescent 2-Styryl Quinolines. *Org Biomol Chem* 2013;11:2597-604.
- [30] a) Schönhaber J, Frank W, Müller TJJ. Insertion–Coupling–Cycloisomerization Domino Synthesis and Cation-Induced Halochromic Fluorescence of 2,4-Diarylpyrano[2,3-*b*]indoles. *Org Lett* 2010;12:4122-5; b) Wilcke T, Glißmann T, Lerch A, Karg M, Müller TJJ. Acidochromic Turn-on 2,4-Diarylpyrano[2,3-*b*]indole Luminophores with Solubilizing Groups for A Broad Range of Polarity. *ChemistrySelect* 2018;3:10345-51.
- [31] Dupeyre G, Lemoine P, Ainseba N, Michel S, Cachet X. A One-pot Synthesis of 7-Phenylindolo[3,2-*a*]carbazoles from Indoles and β -Nitrostyrenes, via an Unprecedented Reaction Sequence. *Org Biomol Chem* 2011;9:7780-90.
- [32] Lane BS, Brown MA, Sames D. Direct Palladium-Catalyzed C-2 and C-3 Arylation of Indoles: A Mechanistic Rationale for Regioselectivity. *J Am Chem Soc* 2005;127:8050-7.
- [33] Guchhait SK, Chaudhary V, Rana VA, Priyadarshani G, Kandekar S, Kashyap M. Oxidative Dearomatization of Indoles via Pd-Catalyzed C–H Oxygenation: An Entry to C2-Quaternary Indolin-3-ones. *Org Lett* 2016;18:1534-7.
- [34] Keith JA, Nielsen RJ, Oxgaard J, Goddard WA. Unraveling the Wacker Oxidation Mechanisms. *J Am Chem Soc* 2007;129:12342-3.
- [35] Taniguchi M, Lindsey JS. Database of Absorption and Fluorescence Spectra of >300 Common Compounds for use in PhotochemCAD. *Photochem Photobiol* 2018;94:290-327.
- [36] Fery-Forgues S, Lavabre D. Are Fluorescence Quantum Yields So Tricky to Measure? A Demonstration Using Familiar Stationery Products. *J Chem Phys* 1999;76:1260.
- [37] Frisch M, Trucks G, B Schlegel B, E Scuseria E, Robb M, Cheeseman J, Scalmani G, Barone V, Mennucci B, A. H. Petersson G, Nakatsuji H, Caricato M, Li X, P Hratchian H, F Izmaylov A, Bloino J, Zheng G, Sonnenberg J, Hada M, Fox D, Gaussian 09 (Revision A02); 2009.
- [38] a) Ernzerhof M, Scuseria GE. Assessment of the Perdew–Burke–Ernzerhof Exchange–Correlation Functional. *J Chem Phys* 1999;110:5029-36; b) Adamo C, Scuseria GE, Barone V. Accurate Excitation Energies from Time-Dependent Density Functional Theory: Assessing the PBE0 model. *J Chem Phys* 1999;111:2889-99.
- [39] a) McLean AD, Chandler GS. Contracted Gaussian Basis Sets for Molecular Calculations. I. Second Row Atoms, Z=11–18. *J Chem Phys* 1980;72:5639-48; b) Krishnan R, Binkley JS, Seeger R, Pople JA. Self-Consistent Molecular Orbital Methods. XX. A Basis Set for Correlated Wave Functions. *J Chem Phys* 1980;72:650-4.
- [40] a) Bauernschmitt R, Ahlrichs R. Treatment of electronic excitations within the adiabatic approximation of time dependent density functional theory. *Chem Phys Lett* 1996;256:454-64; b) Casida ME, Jamorski C, Casida KC, Salahub DR. Molecular Excitation Energies to High-lying Bound States from Time-Dependent Density-Functional Response Theory: Characterization and Correction of the Time-Dependent Local Density Approximation Ionization Threshold. *J Chem Phys* 1998;108:4439-49; c) Stratmann RE, Scuseria GE, Frisch

- MJ. An Efficient Implementation of Time-Dependent Density-Functional Theory for the Calculation of Excitation Energies of Large Molecules. *J Chem Phys* 1998;109:8218-24.
- [41] Scalmani G, Frisch MJ. Continuous Surface Charge Polarizable Continuum Models of Solvation. I. General formalism. *J Chem Phys* 2010;132:114110.
- [42] Lu T, Chen F. Multiwfn: A Multifunctional Wavefunction Analyzer. *J Comput Chem* 2012;33:580-92.
- [43] a) Wang Y, Yang Z, Zhan F, Lyu Z, Han C, Wang X, Chen W, Ding M, Wang R, Jiang Y. Indolizine Quaternary Ammonium Salt Inhibitors part II: A Reinvestigation of an Old-fashioned Strong Acid Corrosion Inhibitor Phenacyl Quinolinium Bromide and its Indolizine Derivative. *New J Chem* 2018;42:12977-89; b) Yang Z, Zhan F, Pan Y, Lyu Z, Han C, Hu Y, Ding P, Gao T, Zhou X, Jiang Y. Structure of a Novel Benzyl Quinolinium Chloride Derivative and its Effective Corrosion Inhibition in 15wt.% Hydrochloric Acid. *Corros Sci* 2015;99:281-94; c) Afarinkia K, Ansari M-R, Bird CW, Gyambibi I. A Reinvestigation of the Structure of the Erythro and Xanthoapocyanine Dyes: Some Unusual Aspects of Quinoline Chemistry. *Tetrahedron Lett* 1996;37:4801-4.
- [44] Caramenti P, Nicolai S, Waser J. Indole- and Pyrrole-BX: Bench-Stable Hypervalent Iodine Reagents for Heterocycle Umpolung. *Chem Eur J* 2017;23:14702-6.
- [45] Chuentragool P, Vongnam K, Rashatasakhon P, Sukwattanasinitt M, Wacharasindhu S. Calcium Carbide as a Cost-effective Starting Material for Symmetrical Diarylethyne via Pd-Catalyzed Coupling Reaction. *Tetrahedron* 2011;67:8177-82.
- [46] Hein SJ, Arslan H, Keresztes I, Dichtel WR. Rapid Synthesis of Crowded Aromatic Architectures from Silyl Acetylenes. *Org Lett* 2014;16:4416-9.

Graphical abstract



Highlights

The urgency and relevance of our contribution for a broad readership of organic, dye and materials chemists is justified by the following aspects:

- 1) Our general approach is the concept of modular one-pot syntheses of functional dyes, predominantly fluorophores. **Indolo[3,2-a]carbazoles** are accessible by a Pd/Cu-catalyzed oxidative four-fold CH-activation that proceeds in a pseudo-threecomponent domino reaction.
- 2) During our methodological studies we not only noticed that the title compounds are intensively **violet to blue emissive in solution and in the solid state**, but also **acidochromic**, i.e. a significant red shift of the absorption bands **with concomitant fluorescence quenching**.
- 3) By comprehensive **NMR studies** the **site of protonation** as assessed, showing that the protonated species falls into the rarely occurring class of apocyanines. The site of protonation was additionally corroborated by **DFT calculations** on various conceivable isomers.
- 4) The isosbestic points in the protonated absorption spectra as well as the static fluorescence quenching (Stern-Vollmer plot) furthermore allows **determining the pK_a** of conjugated acids of the title compounds, i.e. apocyanines.
- 5) The elucidation of the electronic structure by **DFT and TD DFT calculations** using the PBEh1PBE functional reveals that the longest wavelength chromogenic absorption band can be indeed assigned to dominant cyanine like **HOMO-LUMO transitions**.